Sinonasal Inflammation or Neoplasm: Raise the Red Flags!—A Pictorial Review

Jyoti Kumar[1]   Radhika Daga[1]   Gaurav Pradhan[1]   Ravi Meher[2]

[1] Department of Radiodiagnosis, Maulana Azad Medical College &
Associated Hospitals, New Delhi, Delhi, India
[2] Department of Otorhinolaryngology Head and Neck Surgery,
Maulana Azad Medical College & Associated Hospitals, New Delhi,
Delhi, India

Address for correspondence Jyoti Kumar, MD, DNB, Department of
Radiology, Maulana Azad Medical College and Lok Nayak Hospital,
Jawaharlal Nehru Marg, New Delhi 110002, India
(e-mail: drjyotikumar@gmail.com).

Abstract

Keywords
► chronic sinusitis
► sinonasal neoplasms
► red flags
► CT

Inflammatory pathology remains the most common indication for sinonasal imaging. However, sinonasal region is also the epicenter of a variety of neoplasms. These are often missed both clinically and radiologically owing to nonspecific signs and symptoms and subtle imaging pointers. An early diagnosis of sinonasal neoplasms is critical for timely management and hence better prognosis and survival rate.

This pictorial review aims to acquaint the reader with the "red flag" signs on computed tomography that should raise suspicion for an underlying neoplastic pathology and also highlights the imaging features of common sinonasal neoplasms.

Introduction

Sinonasal imaging is primarily done using computed tomography (CT), the most common indication being chronic rhinosinusitis. Polypoidal sinonasal lesions are often a result of inflammatory pathology.

Sinonasal cavity is also the epicenter of a diverse array of neoplasms that are often mistaken for inflammatory disease. As the early presenting symptoms may be nonspecific and imaging findings are often misinterpreted, presence of few clinical red flags may point toward an underlying serious pathology necessitating further workup in these cases. The clinical red flags include:

- Advancing age: Sinonasal neoplasms typically present after the age of 50 years. However, some sinonasal neoplasms are common in the pediatric age group that include rhabdomyosarcoma, esthesioneuroblastoma, nasopharyngeal carcinoma, and lymphoma.

- Alarming clinical symptoms: While presence of rhinorrhea and nasal blockade is nonspecific findings,[1] the presence of 4Ps that include Pain, Paraesthesia, Proptosis, Persistent nasal bleed may point to an underlying grave etiology.

- Clinical examination findings: Irregular, hard, ulceroproliferative lesion that is friable to touch and insensitive to pain is red flag on direct nasal endoscopy. Additionally, presence of accompanying lymphadenopathy would point to an underlying sinister clinical disease.

Although sinonasal neoplasms constitute only approximately 3% of head and neck cancers, more than 50% of malignant neoplasms are diagnosed in an advanced stage with poor prognostic outcome.[2] Awareness of the subtle pointers to an underlying neoplastic process on CT paranasal sinus along with a high index of suspicion is imperative for early diagnosis, which is the most important modifiable factor affecting survival.[2]

Table 1 "Red flag" signs on CT

I	Unilateral sinonasal disease
II	Unilateral olfactory recess involvement
III	Mild hyperdensity on noncontrast CT with solid/heterogeneous enhancement on contrast enhanced scan
IV	Focal hyperostosis
V	Osseous destruction/remodeling
VI	Extrasinus extension
VII	Perineural spread
VIII	Lymphadenopathy

Abbreviation: CT, computed tomography.

This article also depicts the "red flag" signs on CT (►Table 1) that should raise the suspicion of an underlying neoplastic process and warrant further dedicated imaging using magnetic resonance imaging (MRI) that depicts superior contrast resolution.

Unilateral Sinonasal Disease/Single Sinus Disease

Unilateral disease is an uncommon finding and has a variable incidence ranging from 2.5 to 44% in patients undergoing sinonasal imaging.[3–5] Unilateral disease has a greater likelihood of being neoplastic than bilateral disease (►Fig. 1A). In a study by Eckhoff et al,[6] 33.6% of unilateral disease was neoplastic in origin with statistically significant association between unilateral disease and neoplastic etiology. Approximately 95% of bilateral sinonasal disease processes were inflammatory in origin, chronic rhinosinusitis with and without polyposis, and allergic fungal sinusitis accounting for the majority of cases (►Fig. 1B). Unilateral inflammatory masses include polyps, mucocele, and fungal ball. Single sinus disease also has greater chances of an underlying neoplastic process and must be carefully evaluated for additional suspicious features (►Fig. 1C).
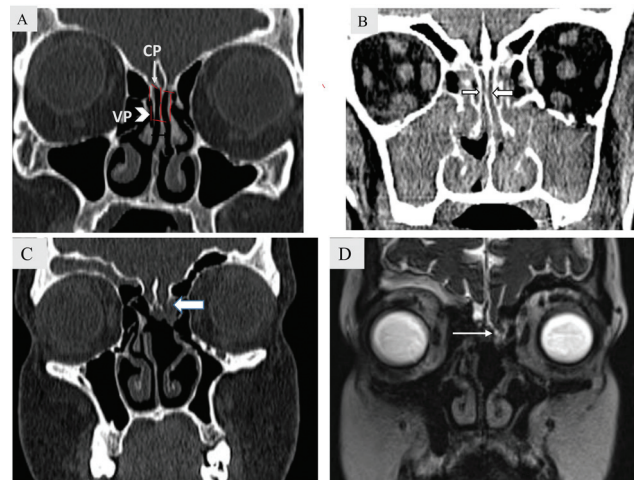

Fig. 2 (A) Olfactory recess anatomy. Coronal bone window computed tomography (CT) image demonstrates olfactory recesses as paired structures (dashed lines) in the roof of the nasal cavity between the nasal septum medially, vertical portion (VP) of the middle turbinate laterally (white arrowhead), and the cribriform plate(CP) superiorly (white arrow). (B) Bilateral olfactory recess opacification in a case of chronic rhinosinusitis. Coronal soft tissue CT image demonstrates diffuse opacification of nasal cavity, bilateral maxillary sinus, and ethmoidal air cells with opacification also noted in bilateral olfactory recesses (block arrow). (C–D): Unilateral olfactory recess opacification in a 20-year-old woman with nasal encephalocele. Coronal bone window (C) CT images shows left olfactory recess opacification with a defect in the cribriform plate (block arrow). Heavily T2-weighted SPACE coronal image (D) depicts the herniation of basifrontal brain parenchyma (white arrow).

Unilateral Olfactory Recess Opacification

Olfactory recesses are paired structures noted in the roof of the nasal cavity between the nasal septum medially, vertical portion of the middle turbinate laterally, and the cribriform plate superiorly (►Fig. 2A, B). However, bilateral olfactory recess opacification occurs mostly with inflammatory sinonasal disease.

Unilateral olfactory recess opacification should be considered suspicious of a more serious pathology. Nondependent polypoidal masses involving the olfactory recess include meningocele/encephalocele (►Fig. 2C, D), sinonasal epithelial
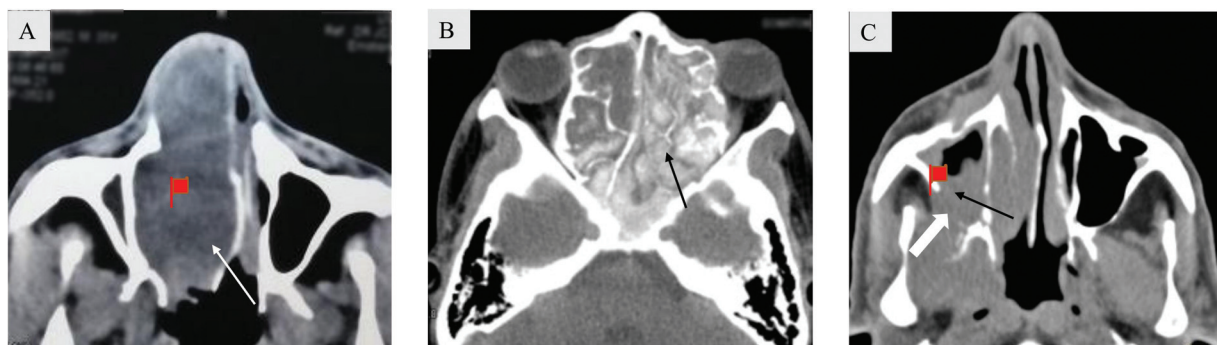

Fig. 1 (A) Unilateral nasal mass. Axial noncontrast computed tomography (NCCT) soft tissue image shows a well-marginated expansile mass in the right nasal fossa (white arrow). Biopsy revealed pleomorphic adenoma. (B) Bilateral sinonasal polypoidal mass. Axial NCCT soft tissue image shows diffuse sinonasal mucosal thickening with expansion and hyperdensities seen within bilateral ethmoidal air cells (black arrow) in a case of allergic fungal sinusitis. (C) Single sinus disease. Axial soft tissue CT image shows a mass in the right maxillary sinus (black arrow) with destruction of posterolateral wall of right maxillary sinus (block arrow). There is extension of the mass into the retromaxillary fat space and loss of fat planes with temporalis and pterygoid muscles. Biopsy revealed adenoid cystic carcinoma.
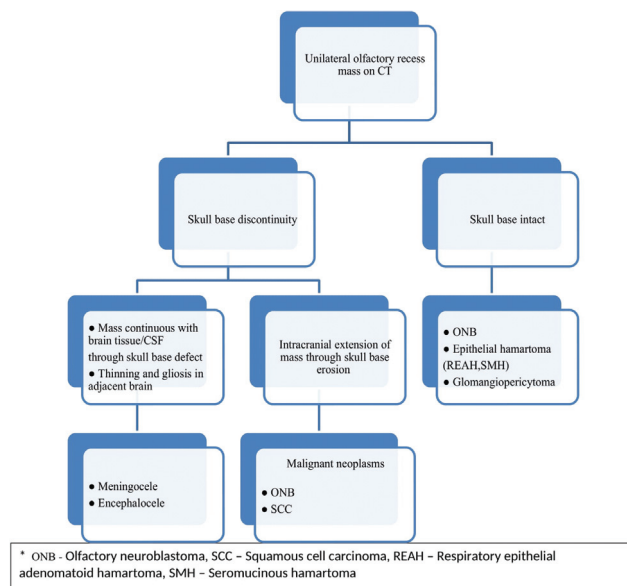
Fig. 3 Analgorithmic approach to differentiate malignant neoplasms from benign masses in the olfactory recess.

hamartoma (respiratory epithelial adenomatoid hamartoma [REAH], seromucinous hamartoma [SMH]), and malignant neoplasm (olfactory neuroblastoma [ONB], epithelial carcinoma). Presence of skull base erosion or defect favors the diagnosis of malignant neoplasm and cephalocele over benign neoplasms and inflammatory polyps. Malignant neoplasms from benign neoplasms in the olfactory recess is depicted in ►Fig 3.

ONB (►Fig. 4) originates in the olfactory recess with a propensity for extranasal spread. Intracranial extension is common and gives "dumbbell" or "figure of 8" shape to the mass with erosion of cribriform plate (►Fig. 4B, C). Although not very commonly seen, cyst at the tumor brain interface is a distinguishing feature (►Fig. 4D).[7]

Sinonasal epithelial hamartomas (REAH, SMH) are seen as homogeneously enhancing masses expanding the olfactory cleft without accompanying bone destruction.

Mild Hyperdensity on Noncontrast CT with Solid/Heterogeneous Enhancement on Contrast Enhanced Scan

Neoplasms are generally mildly hyperdense on noncontrast CT (NCCT) and depict solid enhancement on contrast administration (►Fig. 5). Inflammatory polypoidal masses are usually hypodense and show either no enhancement or thin linear peripheral enhancement. Proteinaceous secretions and fungal infection are benign causes of hyperdensity on a NCCT that is usually greater than that seen in a neoplastic process (►Fig. 1B).

Small neoplastic masses are usually homogeneous, whereas large masses are more heterogeneous with areas of necrosis and hemorrhage as they enlarge to outgrow their vascular supply. Squamous cell carcinoma (SCC) is the most common malignant neoplasm involving the sinonasal region and shows characteristic necrosis when large (►Fig. 6). However, lymphoma typically remains a homogeneous mass despite its bulky tumor volume. The mean apparent diffusion coefficient
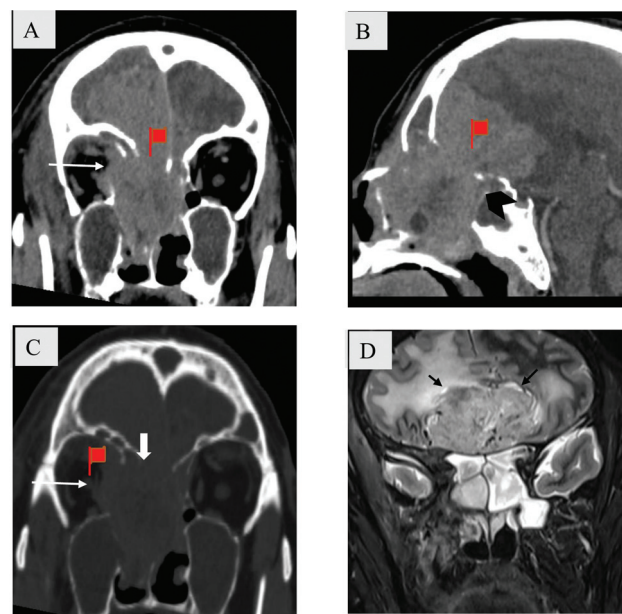

Fig. 4 (A–D) Olfactory recess mass with bone destruction in a 55-year-old man with olfactory neuroblastoma. Coronal (A), sagittal (B) soft tissue and coronal bone window. (C) Computed tomography images show a large ill-defined heterogeneously enhancing solid mass in the superior nasal cavity and bilateral ethmoidal air cells. There is destruction of cribriform plate (block arrow), fovea ethmoidalis, and lamina papyracea with involvement of medial rectus muscle (white arrow). (D) There is intracranial extension of the mass giving "dumbbell/ Fig. of 8" appearance (black arrowhead) with small cysts at tumor brain interface seen on coronal T2-weighted magnetic resonance (black arrow).
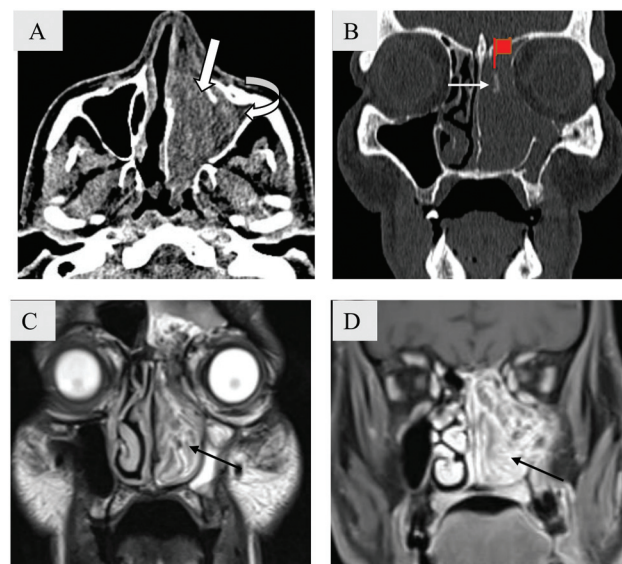

Fig. 5 Focal hyperostosis in a 61-year-old man with inverted papilloma. Axial soft tissue (A) and coronal bone window CT images (B) show hyperdense mass in the left nasal cavity and maxillary sinus (block arrow) with hypodense fluid attenuation noted in the periphery of the mass (curved arrow) s/o retained secretions. There is bowing of the medial wall of left maxillary sinus laterally. An area of focal hyperostosis is seen in left superior nasal cavity (white arrow). Coronal T2-weighted (T2W; C) and T1W post contrast magnetic resonance images (D) show classical convoluted cerebriform pattern seen as alternatively low and high intensity bands (black arrow).
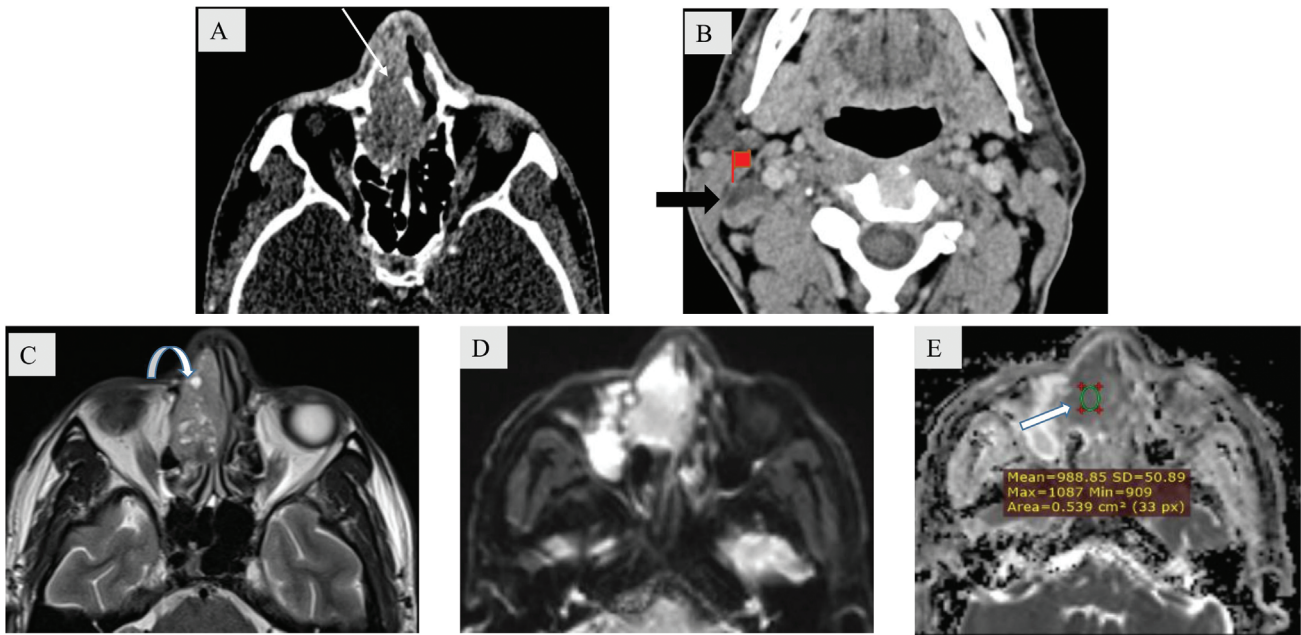
Fig. 6 A 68-year-old male patient with squamous cell carcinoma. Axial soft tissue (**A**) window computed tomography (CT) image shows a heterogeneous mass within the right nasal cavity and ethmoidal air cells (white arrow). Axial soft tissue (**B**) window CT image shows a heterogeneous right level II cervical lymph node noted with eccentric focus of necrosis (block arrow). The necrotic areas are distinctly depicted on T2-weighted axial magnetic resonance image (curved arrow) (**C**). Diffusion-weighted imaging/ apparent diffusion coefficient (DWI/ADC) mapping (**D, E**) depicts restricted diffusion with mean ADC value approximately 0.988×10^{-3} mm^2/sec (block arrow).

value in lymphoma is lower ($\sim 0.59 \times 10^{-3}$ mm^2/sec) than in SCC (0.97×10^{-3} mm^2/s).[8]

Focal Hyperostosis

Focal hyperostosis is a localized area of bony thickening that is a hallmark of inverted papilloma (IP) when seen.

IP is the most common benign epithelial neoplasm of the sinonasal region characteristically located in the lateral nasal cavity in the region of middle turbinate or medial wall of maxillary sinus. Although it most often results in expansion and remodeling of the adjacent bone, it may result in bone destruction as it enlarges. The site of focal hyperostosis represents the site of origin of the neoplasm and needs to be removed during surgery, as inadequate removal is a major contributor of recurrence (►**Fig. 5A, B**).

A close differential on NCCT is an antrochoanal polyp as both lesions have the same location and cause underlying bony remodeling. Intralesional calcific foci/bone destruction when present and solid enhancement on contrast administration can suggest the correct diagnosis of IP. Convoluted cerebriform pattern seen on MR has a diagnostic accuracy of 89% for IP (►**Fig. 5C, D**).[9]

Osseous Changes

Osseous lytic destruction is a feature typical of sinonasal neoplasm (►**Fig. 7**). Key bony structures to evaluate are bony orbital walls, cribriform plate, fovea ethmoidalis, posterior wall
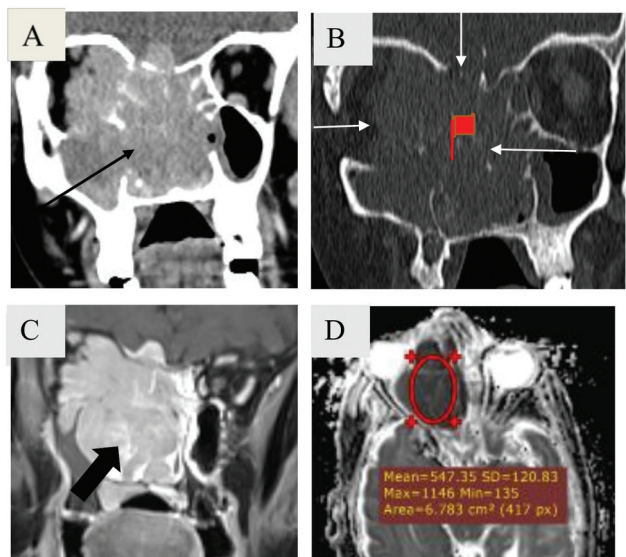

Fig. 7 Bone destruction in a 63-year-old female patient with large B cell non-Hodgkin lymphoma. Coronal soft tissue (**A**) and bone window (**B**) computed tomography images reveal a large relatively homogeneous mass (black arrow) involving nasal cavity, bilateral ethmoidal air cells, right maxillary sinus, right orbit, right basifrontal region with extensive bone destruction (white arrows). Magnetic resonance imaging depicts homogeneous post contrast enhancement (block arrow) and marked diffusion restriction. Note that mean apparent diffusion coefficient (ADC) value $\sim 0.54 \times 10^{-3}$ mm^2/sec is much lower than that of squamous cell carcinoma (ADC value: $\sim 0.988 \times 10^{-3}$ mm2/sec) in ►**Fig. 5**. The mass is homogeneous despite its bulk.
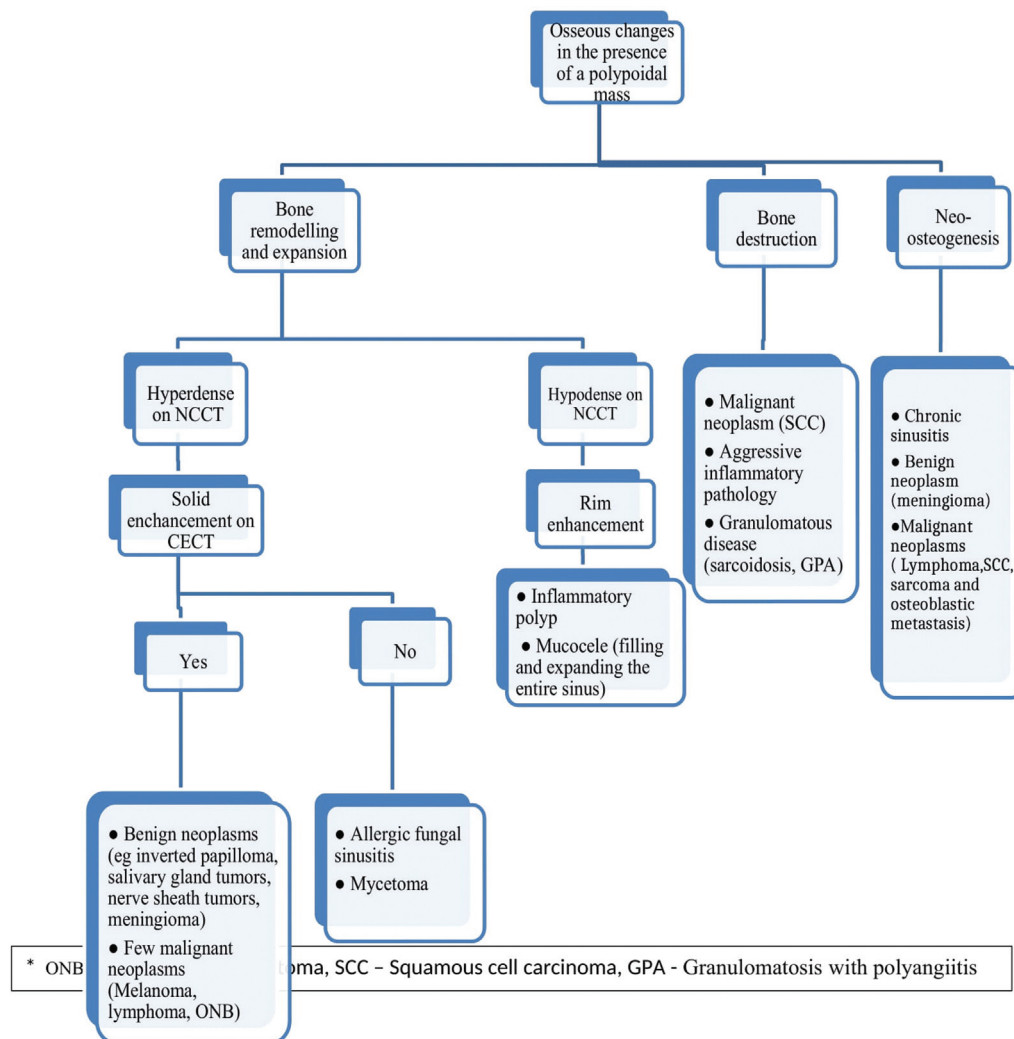
Fig. 8 Algorithmic approach to a sinonasal polypoidal mass based on accompanying osseous changes.

of maxillary sinus, pterygopalatine fossa, pterygoid plates, walls of sphenoid sinus, and posterior table of frontal sinus.

Destruction of the posterolateral maxillary sinus wall is considered diagnostic of a neoplastic process (►**Fig. 1C**).[10] An algorithmic approach to differentiate sinonasal pathologies based on pattern of bone involvement is depicted in ►**Fig 8**.

Expansile remodeling with pressure erosion is seen with slow growing benign neoplasms (IP [►**Fig. 5**], pleomorphic adenoma, juvenile nasopharyngeal angiofibroma, schwannoma) as well as chronic expansile inflammatory conditions (mucocele [►**Fig. 9**] and antrochoanal polyp).

However, there are exceptions to the rule. A few malignant neoplasms like large cell lymphoma, melanoma (►**Fig. 10**), low-grade minor salivary gland malignancy, extramedullary plasmacytoma, sarcoma, and ONB may predominantly result in bone expansion and remodeling. In these cases, other red flag signs including unilateral opacification and mild hyperdensity on NCCT are subtle clues that warrant further investigation.

On the other hand, a few benign conditions like invasive fungal sinusitis, granulomatous diseases (granulomatosis with polyangiitis and sarcoidosis), and giant cell reparative
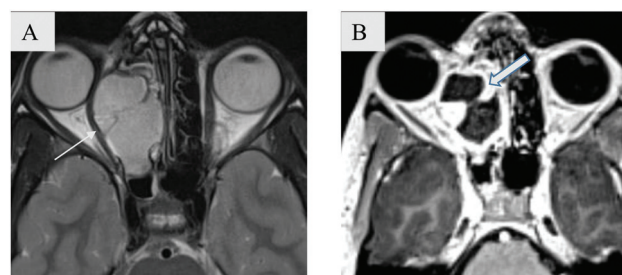

Fig. 9 Bone expansion with rim enhancement in a 14-year-old adolescent female patient with ethmoidal mucocele. Axial T2-weighted imaging (T2WI) (**A**) and post-contrast T1WI (**B**) images show well marginated lobulated lesion in right ethmoidal air cells causing its expansion with extraconal extension into the right orbit and stretching of right medial rectus (white arrow). The lesion shows septation within and peripheral rim.

granuloma can result in aggressive bone destruction (►**Fig. 11**).[10]

Sclerotic bony change/neo-osteogenesis is typically seen in a chronic inflammatory process (►**Fig. 12**). However, neoplasms that can depict bone sclerosis include sinonasal
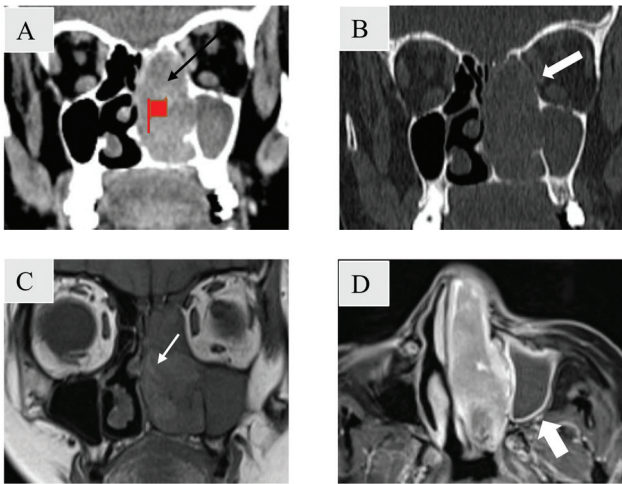
Fig. 10 Bone remodeling and destruction in a 60-year-old female patient with melanoma. Coronal soft tissue (**A**) and bone window (**B**) computed tomography images show a unilateral mildly enhancing mass involving left nasal cavity and ethmoidal air cells (black arrow) with adjacent bone remodeling seen as bowing of nasal septum and left lamina papyracea (block arrows). Left sided turbinates are destroyed. On coronal T1-weighted magnetic resonance imaging (MRI) (**C**), a characteristic septate pattern owing to alternate hypo and hyperintense striations is seen (white arrow). The mass in the nasal cavity shows heterogeneous enhancement with peripherally enhancing entrapped secretions seen in the left maxillary sinus on post contrast T1-weighted MRI (white block arrow) (**D**).

meningioma and lymphoma. Rarely, SCC sarcoma and osteoblastic metastases can also show bone sclerosis.

Extrasinus Extension

Extrasinus extension into surrounding soft tissues, orbit, and cranium is characteristic of sinonasal malignant neoplasms and affects the staging of the tumor. Extrasinus extension can often occur in a continuous manner at the site of bone destruction or as perineural spread. Lymphoma is a malignancy that can involve extrasinus fat and soft tissue without bone destruction. This appearance can also be seen in aggressive inflammatory pathology such as acute invasive fungal sinusitis seen in the immunocompromised and granulomatous diseases like sarcoidosis.

MR is a more sensitive modality than CT to detect orbital invasion (►**Fig. 13**), as loss of integrity of bony orbit on CT is
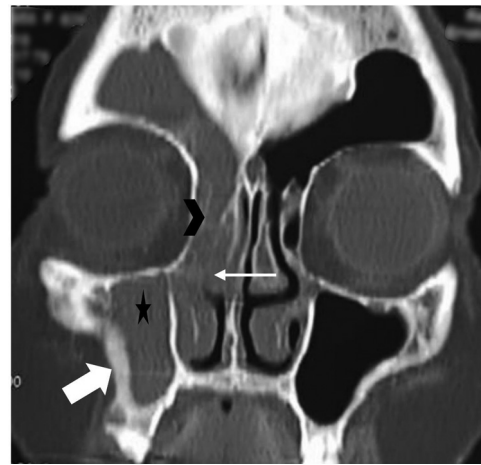

Fig. 12 Sclerotic bone changes in a 60-year-old female patient with chronic rhinosinusitis. Coronal bone window computed tomography image shows unilateral opacification of right maxillary sinus (asterisk), middle meatus (white arrow), anterior ethmoidal air cells (arrowhead), and right frontal sinus with bony sclerosis (block arrow) involving right maxillary antral wall s/o ostiomeatal pattern of chronic sinusitis.

not a definitive sign of orbital invasion. Extension of tumor beyond the periorbita (T2 hypointense rim) or tumor-periorbital nodular interface on MR are early signs of orbital invasion. Extraocular muscle enlargement is the most specific parameter for intraorbital extension and is seen well on both CT and MR.[11]

Erosion of bony calvarial wall with infiltration in the adjacent brain parenchyma, nodular dural enhancement, dural thickening more than or equal to 5 mm, absence of the T2 hypointense zone (dura), and pial involvement are the best predictors on imaging to assess for intracranial extension (►**Fig. 14A, B**).[10] Presence of thin linear dural enhancement is not a remarkable predictor for dural invasion (►**Fig. 14C**). Intraoperative frozen section evaluation remains the key to confirm diagnosis of orbital/intracranial extension.

Perineural Spread

Perineural spread implies neoplastic extension using the nerve as a scaffold.

Fig. 11 Extrasinus extension in a 53-year-old male patient with acute invasive fungal sinusitis. Axial (**A**), coronal (**B**), and sagittal (**C**) soft tissue computed tomography images show circumferential soft tissue thickening involving right maxillary antrum with destruction of the anterior and posterior walls of maxillary sinus and extension into the prenatal (arrowhead) and retromaxillary fat (black arrow). The lesion is also seen to destroy the floor of the right orbit with intra-orbital extension (white arrow).
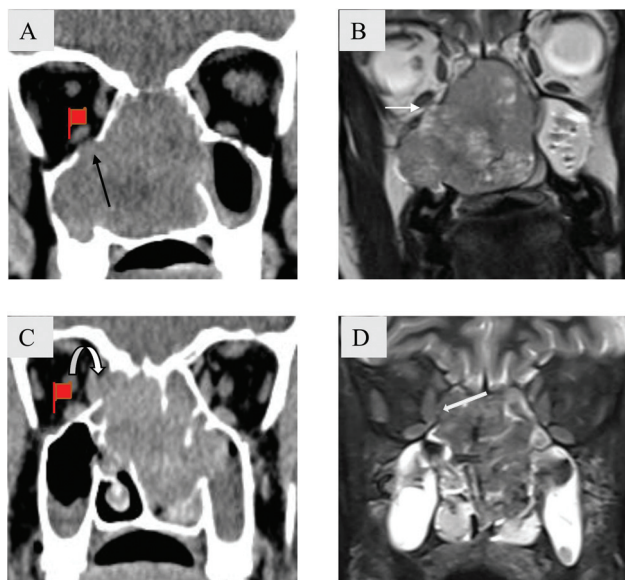
Fig. 13 Imaging features of orbital invasion. A 27-year-old female patient with adenoid cystic carcinoma. Coronal soft tissue (**A**) computed tomography (CT) image shows expansion and complete opacification of the nasal cavity, bilateral ethmoidal air cells and right maxillary sinus. There is destruction of inferior wall of right orbit with suspicious area of intraorbital extension (black arrow). Intact periorbita seen as a hypointense line (white arrow) on T2-weighted magnetic resonance imaging (T2W MRI) (**B**) confirms that there is no orbital invasion. (**C, D**): A 48-year-old man with adenocarcinoma. Coronal soft tissue (**C**) CT image shows an ill-marginated mildly heterogeneously enhancing mass centered in bilateral ethmoidal air cells and nasal cavity. There is destruction of right lamina papyracea with loss of fat planes with the medial rectus muscle (curved arrow). Coronal T2W MRI (**D**) reveals discontinuity of the right periorbita (block arrow) favoring intraorbital extension.

Table 3 Key areas to evaluate perineural spread

Cranial nerve	Area
V	Meckel's cave
V1	Fat pad superior to the levator palpebrae muscle
	Fat pad anterior to superior orbital rim
V2	Fat in pterygopalatine fossa
	Preantral and postantral fat pads
V3	Fat pad at foramen ovale
	Fat pad at mandibular foramen
	Mandibular bone marrow fat
	Fat pad anterior to the mental foramen
	Muscles of mastication (particularly pterygoid, masseter and superficial temporal muscles)
VII	Fat pad at stylomastoid foramen

It carries a poor prognosis and also impacts management decisions. It is associated with an increased risk of recurrence and reduced 5-year survival rate by up to 30%.[12]

Since approximately 40% of the patients with perineural spread are completely asymptomatic.[13] The radiologist may be the first to detect it.

Although MRI is a more sensitive tool than CT to detect perineural spread, various primary and secondary signs (►Table 2) can be picked on CT, when keeping a high index of suspicion while evaluating the key areas (►Table 3; ►Figs. 15–16).
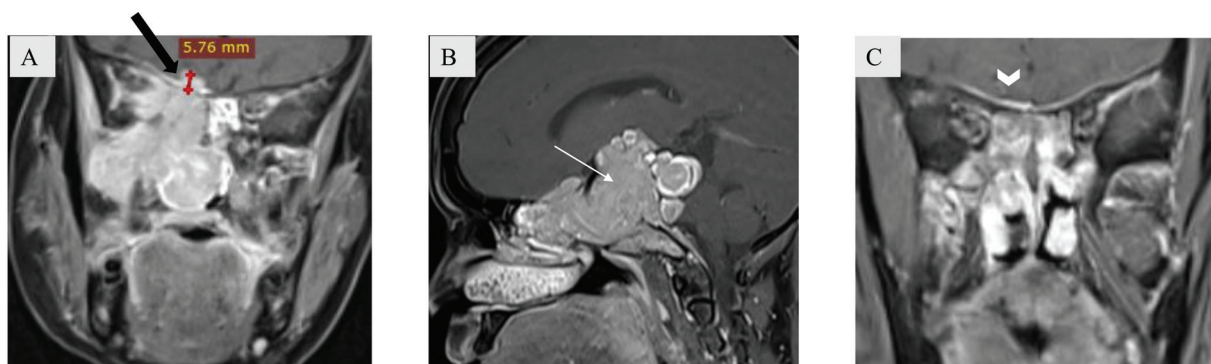

Fig. 14 (**A–C**) Patterns of dural enhancement on postcontrast T1-weighted coronal images. Nodular dural enhancement measuring more than 5 mm in maximum thickness (block arrow in A) and frank intracranial infiltration (white arrow in B) are considered main indicators of intracranial extension. Linear dural enhancement (arrowhead in C) is not confirmatory for intracranial extension.

Table 2 Signs of perineural spread

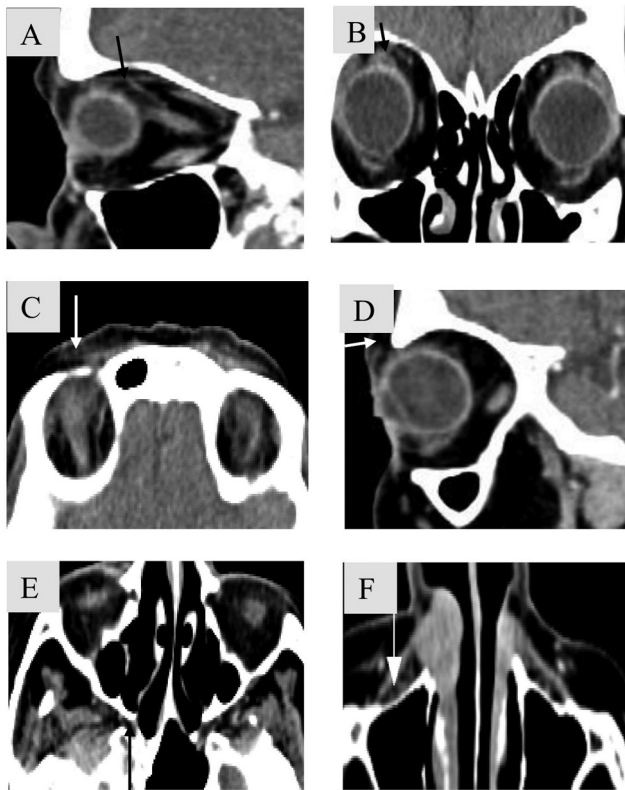| Primary	Secondary
Loss of fat within neural foramina or PPF	Denervation atrophy of the innervated muscles
Widening or destruction of neural foramina	-Acute to subacute (edema with increased enhancement)
Excessive enhancement within the foramina/ cavernous sinus/PPF or Meckel's cave	-Chronic (atrophy)

Abbreviation: PPF, pterygopalatine fossa.

Fig. 15 Key areas for the evaluation of perineural spread along V1, V2. Cranial nerve (CN) V1 (**A, B**). Fat pad superior to levator palpebrae superioris muscle (black arrow). (**C, D**). Fat pad anterior to superior orbital rim (white arrow). CN V2 (**E**). Fat in pterygopalatine fossa (black arrow). **F**. Preantral fat pad (white arrow).

The common malignant sinonasal neoplasms to depict perineural spread include adenoid cystic carcinoma (►Fig. 17), SCC, mucoepidermoid carcinoma, desmoplastic melanoma, and lymphoma. Risk factors include male gender, increasing tumor size, recurrent tumor, and poor histological differentiation.[14] Although any cranial nerve may be affected, the trigeminal (CN5) and facial (CN7) nerves are most commonly involved owing to their extensive innervation in the head and neck region. Usually, the spread pattern is centripetal toward the brain; however, centrifugal spread is also seen.

Perineural spread is not always associated with malignant neoplasms. Inflammatory disorders like invasive fungal disease and sarcoidosis are the benign conditions that can spread along the nerves. Other mimics include primary neurogenic tumors such as schwannomas and meningioma that may be seen herniating through skull base foramina.

Lymphadenopathy

Lymph node enlargement in the presence of a sinonasal polypoidal lesion favors the diagnosis of malignancy. The most common lymph nodes involved are level I, II and retropharyngeal nodes (►Fig. 6B). The neoplasms most commonly associated with lymph node metastasis include sinonasal undifferentiated carcinoma, SCC, ONB, neuroendocrine carcinoma and soft tissue carcinoma, while adenoid
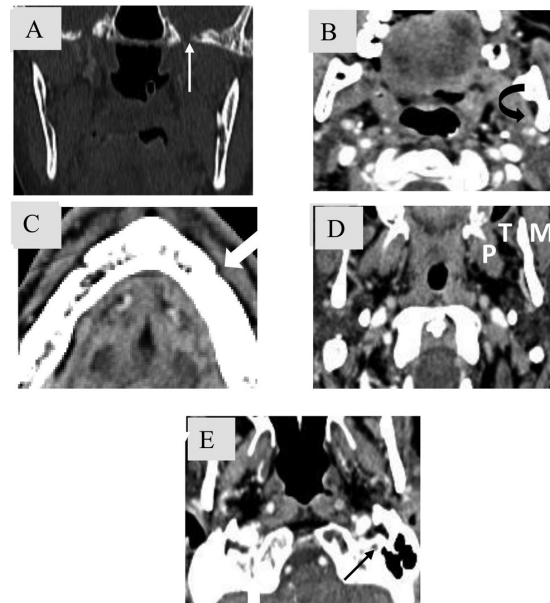

Fig. 16 Key areas for the evaluation of perineural spread along V3 and VII cranial nerve (CN). CN V3 (**A**) Foramen ovale. (**B**) Fat pad in mandibular foramen. (**C**) Fat pad anterior to mental foramen. (**D**) Muscles of mastication (pterygoid (P), masseter (M) and superficial temporalis (T) muscles. CN VII (**E**) Fat pad at stylomastoid foramen.
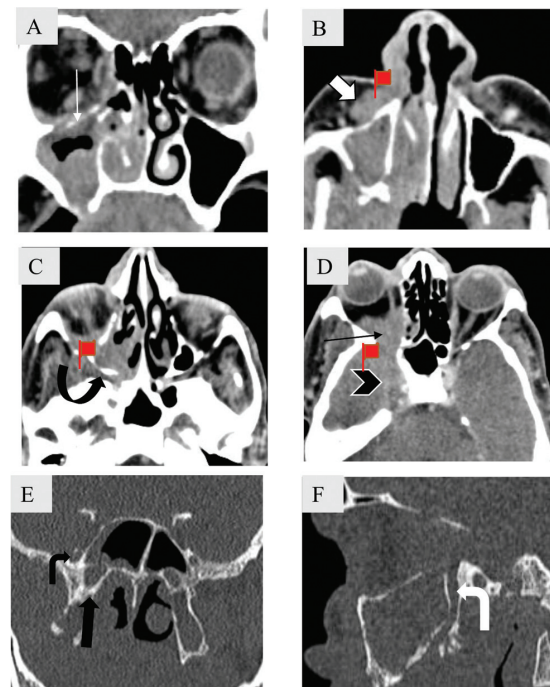

Fig. 17 Perineural spread along V2 in a 62-year-old male patient with adenoid cystic carcinoma of maxillary sinus. Coronal (**A**) and axial soft tissue computed tomography (CT) images (**B–D**) caudal to cranial show homogenously enhancing mass seen involving the right maxillary sinus with destruction and enlargement of right infraorbital canal (white arrow) with soft tissue extension into the preantral fat (block arrow). Soft tissue is seen to extend into the pterygopalatine fossa (curved arrow) and the orbit (black arrow) through the inferior orbital fissure. Centripetal extension in the cavernous sinus is also noted (arrowhead). Coronal (**E**) and sagittal bone (**F**) window CT images depict enlarged right foramen rotundum (bent black arrow) and vidian canal (asterisk). Right greater palatine is also enlarged.

cystic carcinoma and adenocarcinoma are least commonly associated.[15]

Although predictive value of these red flag signs on NCCT is not known, El-Gerby and El-Anwar[16] found that unilateral sinus involvement, bone involvement, tumor necrosis, soft tissue mass, lymphadenopathy, and involvement of surrounding structures on MRI had a combined positive predictive value and negative predictive value of 62.5 and 87%, respectively, in differentiating benign from malignant sinonasal neoplasms.

Tumor Mimics

Few inflammatory pathologies can mimic neoplasms, both can be very aggressive on imaging (►Fig. 18) and awareness of these entities with their distinguishing imaging features is useful in discriminating between the two groups as depicted in ►Table 4.

Conclusion

CT of sinonasal region is a routine investigation done for inflammatory pathology. Although neoplasms of the region are uncommon, they are often missed owing to nonspecific clinical presentation and subtle imaging findings that go undetected. Awareness of CT "red flags" that suggest the possibility of an underlying neoplastic etiology in early stages of the disease can be extremely useful in reducing the morbidity and mortality associated with sinonasal neoplasms.
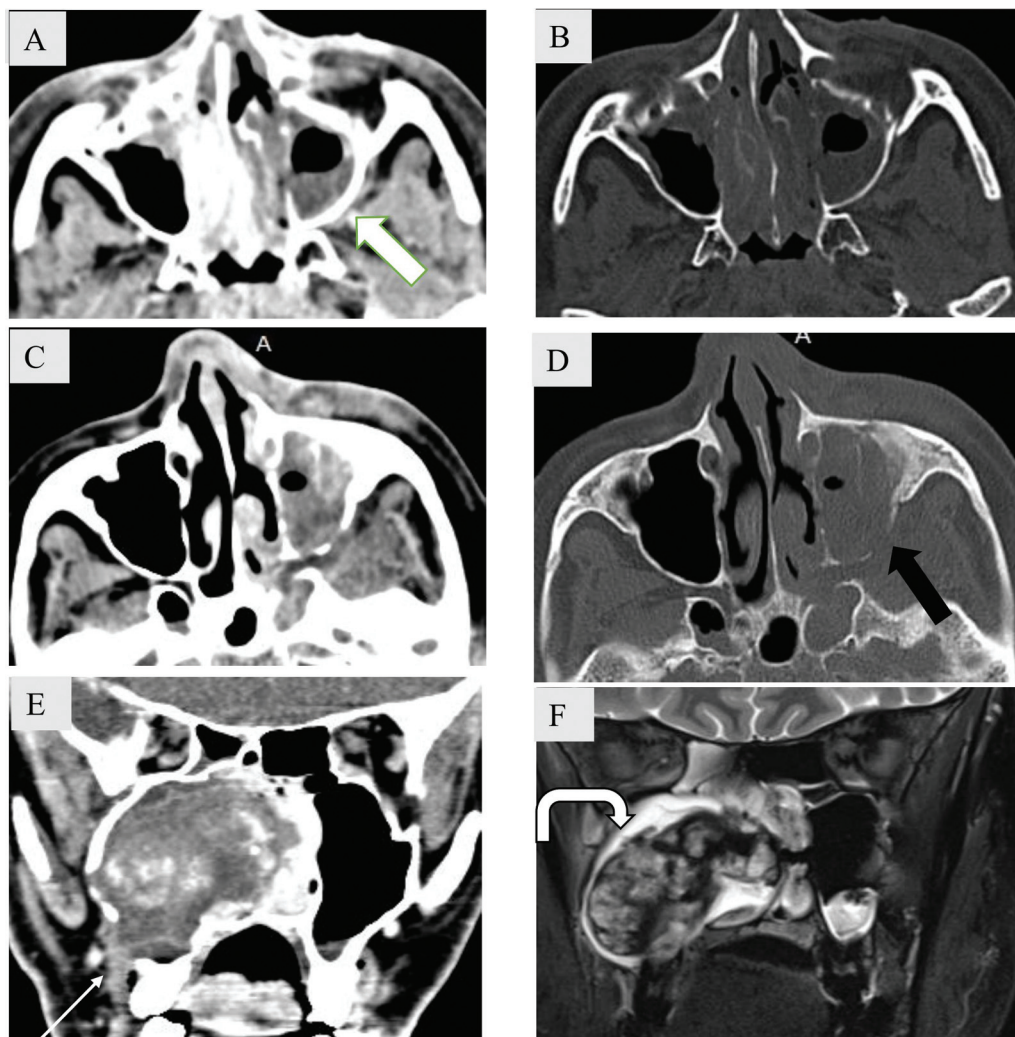

Fig. 18 Tumor mimics: Extrasinus extension in acute invasive fungal rhinosinusitis without bony erosion (A-B) and with bony erosion (C–D). Axial noncontrast computed tomography (NCCT) soft tissue and bone window images (A–B) show partial opacification of left maxillary sinus with extension of the soft tissue into retroantral space (white block arrow) without any bony erosion. Axial NCCT soft tissue and bone window images (C, D) show near complete opacification of left maxillary sinus with destruction of posterolateral wall (black arrow) and extrasinus extension into the periantral space and pterygopalatine fossa. (E–F) Coronal soft tissue CT image (E) shows an expansile mass in the right maxillary sinus with amorphous hyperdense areas within. Cortical breach is noted along the inferolateral wall with extrasinus extension (white arrow). T2-weighted coronal magnetic resonance imaging (F) shows lobulated mass with T2 hypointense fibrous capsule (curved arrow). Biopsy revealed sinonasal organized hematoma.

Table 4 Non-neoplastic lesions mimicking sinonasal malignancies

Conditions	Differentiating imaging features
Chronic invasive fungal sinusitis	• Seen in immunocompetent/ mildly immunocompromised individuals • Homogeneous contrast enhancement of the involved sinus with relative lack of expansion • Extrasinus extension and bone erosions; sclerotic changes may be seen that reflect chronicity • Marked hypointense signal on T2-weighted images
Acute invasive fungal rhinosinusitis	• Seen in immunocompromised individuals • Rapid, progressive extrasinus extension with/without bone erosions owing to spread along the neurovascular channels • Isohypointense signal on T2-weighted images • Absent enhancement suggests necrosis
IgG4-related disease	• Seen in elderly • Homogeneous soft tissue lesion with/without bone erosions • Hypointense signal on T2-weighted images • Homogeneous contrast enhancement may show heterogeneous areas due to dense fibrosis • Perineural spread with predilection for infraorbital branch of trigeminal nerve • Other systemic manifestations of IgG4 disease such as Riedel thyroiditis, fibrosing mediastinitis, autoimmune pancreatitis, sclerosing cholangitis, retroperitoneal fibrosis may be present with raised serum IgG4 levels
Sinonasal organized hematoma	• Seen in second-eighth decade • Expansile soft tissue mass with remodeling and pressure erosion of bone • Commonly seen in maxillary sinus • Peripheral rim of hypointensity (representing fibrous pseudocapsule) on T2-weighted images • Heterogeneous/frond like contrast enhancement
Granulomatosis with polyangiitis	• Seen at any age but common in fourth-fifth decade of life • Mucosal thickening with bone erosions and neo-osteogenesis Nasal septal perforation and turbinate erosions are characteristic • Hypointense signal on T2-weighted images • Heterogeneous contrast enhancement • Classic triad includes involvement of lungs, upper respiratory tract and kidneys with c-ANCA positive in 90% cases

Abbreviations: c-ANCA, Antineutrophil Cytoplasmic Autoantibody, Cytoplasmic; IgG4, immunoglobulin G4.

References

1 Shuaibu IY, Usman MA, Ajiya A. Unilateral sinonasal masses: Review of clinical presentation and outcome in Ahmadu Bello university teaching hospital, Zaria, Nigeria. Niger Med J 2020;61(01):16–21

2 Bhattacharyya N. Factors affecting survival in maxillary sinus cancer. J Oral Maxillofac Surg 2003;61(09):1016–1021

3 Ahsan F, El-Hakim H, Ah-See KW. Unilateral opacification of paranasal sinus CT scans. Otolaryngol Head Neck Surg 2005; 133(02):178–180

4 Lee JY. Unilateral paranasal sinus diseases: analysis of the clinical characteristics, diagnosis, pathology, and computed tomography findings. Acta Otolaryngol 2008;128(06):621–626

5 Beswick DM, Mace JC, Chowdhury NI, et al. Comparison of surgical outcomes between patients with unilateral and bilateral chronic rhinosinusitis. Int Forum Allergy Rhinol 2017;7(12):1162–1169

6 Eckhoff A, Cox D, Luk L, Maidman S, Wise SK, DelGaudio JM. Unilateral versus bilateral sinonasal disease: Considerations in differential diagnosis and workup. Laryngoscope 2020;130(04):E116–E121

7 Dublin AB, Bobinski M. Imaging characteristics of olfactory neuroblastoma (esthesioneuroblastoma). J Neurol Surg B Skull Base 2016;77(01):1–5

8 Kim SH, Mun SJ, Kim HJ, Kim SL, Kim SD, Cho KS. Differential diagnosis of sinonasal lymphoma and squamous cell carcinoma on CT, MRI, and PET/CT. Otolaryngol Head Neck Surg 2018;159(03):494–500

9 Jeon TY, Kim HJ, Chung SK, et al. Sinonasal inverted papilloma: value of convoluted cerebriform pattern on MR imaging. Am J Neuroradiol 2008;29(08):1556–1560

10 Sen S, Chandra A, Mukhopadhyay S, Ghosh P. Imaging approach to sinonasal neoplasms. Neuroimaging Clin N Am 2015;25(04):577–593

11 Eisen MD, Yousem DM, Loevner LA, Thaler ER, Bilker WB, Goldberg AN. Preoperative imaging to predict orbital invasion by tumor. Head Neck 2000;22(05):456–462

12 Moreira MCS, Dos Santos AC, Cintra MB. Perineural spread of malignant head and neck tumors: review of the literature and analysis of cases treated at a teaching hospital. Radiol Bras 2017; 50(05):323–327

13 Dankbaar JW, Pameijer FA, Hendrikse J, Schmalfuss IM. Easily detected signs of perineural tumour spread in head and neck cancer. Insights Imaging 2018;9(06):1089–1095

14 Paes FM, Singer AD, Checkver AN, Palmquist RA, De La Vega G, Sidani C. Perineural spread in head and neck malignancies: clinical significance and evaluation with 18F-FDG PET/CT. Radiographics 2013;33(06):1717–1736

15 Peck BW, Van Abel KM, Moore EJ, Price DL. Rates and locations of regional metastases in sinonasal malignancies: the Mayo Clinic experience. J Neurol Surg B Skull Base 2018;79(03):282–288

16 El-Gerby KM, El-Anwar MW. Differentiating benign from malignant sinonasal lesions: Feasibility of diffusion weighted MRI. Int Arch Otorhinolaryngol 2017;21(04):358–365